Molecular Crystals and Liquid Crystals

Publication details, including instructions for authors and subscription information:
http://www.tandfonline.com/loi/gmcl20

A Study on MgO Characteristics of AC Plasma Display Panel Fabricated by Vacuum Sealing Method

Choon-Sang Park [a], Heung-Sik Tae [a], Young-Kuk Kwon [b] & Eun Gi Heo [b]

[a] School of Electrical Engineering and Computer Science, Kyungpook National University, Daegu, Korea

[b] R&D Team, PDP Division, Samsung SDI Co., Ltd., Cheonan, Korea

Version of record first published: 18 Mar 2009

To cite this article: Choon-Sang Park, Heung-Sik Tae, Young-Kuk Kwon & Eun Gi Heo (2009): A Study on MgO Characteristics of AC Plasma Display Panel Fabricated by Vacuum Sealing Method, Molecular Crystals and Liquid Crystals, 499:1, 224/[546]-233/[555]

To link to this article: http://dx.doi.org/10.1080/15421400802619883

Mol. Cryst. Liq. Cryst., Vol. 499, pp. 224/[546]–233/[555], 2009

ISSN: 1542-1406 print/1563-5287 online
DOI: 10.1080/15421400802619883

Taylor & Francis
Taylor & Francis Group

A Study on MgO Characteristics of AC Plasma Display Panel Fabricated by Vacuum Sealing Method

Choon-Sang Park[1], Heung-Sik Tae[1], Young-Kuk Kwon[2], and Eun Gi Heo[2]
[1]School of Electrical Engineering and Computer Science, Kyungpook National University, Daegu, Korea
[2]R&D Team, PDP Division, Samsung SDI Co., Ltd., Cheonan, Korea

In this paper, the vacuum sealing method to enhance a base vacuum level was adopted, and the resultant changes in the MgO characteristics, such as firing voltage, MgO sputtering rate, MgO hardness, and photoluminescence, were examined in comparison with those in the conventional sealing method in the 42-in. AC-PDP with a high Xe (15%) content. The 42-in. panel fabricated by the vacuum sealing method caused the changes in the MgO characteristics, such as firing voltage, MgO sputtering rate, MgO hardness, and photoluminescence, which are caused by an increase in the oxygen vacancy of the MgO layer.

Keywords: 42-in. AC-PDP module; firing voltage; focused ion beam; MgO hardness; MgO sputtering rate; nanoindentor; oxygen vacancy; photoluminescence; vacuum sealing method; V_t closed curve

1. INTRODUCTION

It is well known that if the base vacuum level before filling a discharge gas is higher, the address and sustain discharge characteristics can be improved in an AC-PDP [1–6]. This improvement may be deeply related to the variation in the MgO surface characteristics depending on the base vacuum level. However, the MgO characteristics in a panel fabricated by the vacuum sealing method are not still fully investigated yet. This paper focuses on the MgO characteristics of the 42-in. panels fabricated by two different sealing methods, such as the conventional and vacuum sealing methods. In the conventional sealing method, the front and rear glasses

This work was supported in part by the Samsung SDI and in part by the Brain Korea 21 (BK21).

Address correspondence to Prof. Heung-Sik Tae, School of Electrical Engineering and Computer Science, Kyungpook National University, Sangyuk-dong, Buk-gu, Daegu 702-701, Korea (ROK). E-mail: hstae@ee.knu.ac.kr

are sealed under the atmospheric pressure (about 760 Torr), whereas in the vacuum sealing method, the front and rear glasses are sealed under a high vacuum chamber (about 10^{-5} Torr). In this paper, the vacuum sealing method is adopted to enhance the base vacuum level. The resultant changes in the MgO characteristics, such as firing voltage, MgO sputtering rate, MgO hardness, and photoluminescence, were examined in comparison with those in the conventional sealing method in the 42-in. AC-PDP with a high Xe (15%) content and a box-type barrier.

2. EXPERIMENTAL SETUP FOR VACUUM SEALING PROCESS

Figure 1 shows the schematic diagram and the sealing process of the 42-in. AC-PDP panel fabricated by the conventional sealing process.

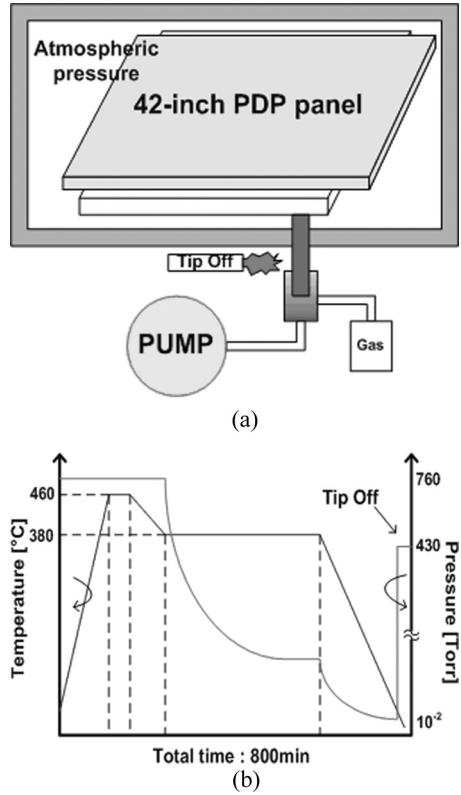

FIGURE 1 (a) Schematic diagram of conventional sealing process, and (b)sealing temperature and corresponding pressure profile during conventional sealing process.

As shown in Figure 1(b), in the conventional sealing method, the front and rear glasses were sealed under atmospheric pressure (about 760 Torr). Then, the panel is evacuated by a high vacuum pump through a glass tip sealed to a corner of rear glass. The resultantly obtained base vacuum level is limited by the pumping conductance of the panel, mainly attributed by the barrier shape. In the conventional sealing method with a box type barrier, the base vacuum level at a center region and a region located far away from the glass tip in the 42-in. panel was obtained by about 10^{-2} Torr [5]. Figure 2 shows the

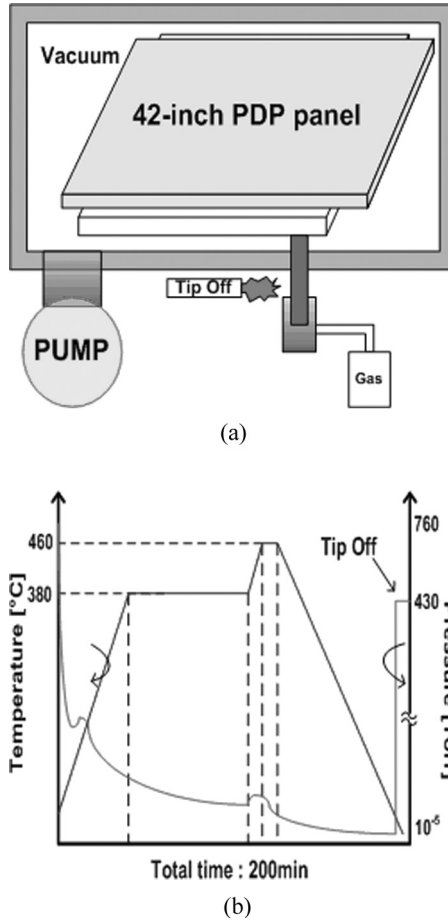

FIGURE 2 (a) Schematic diagram of vacuum sealing process, and (b) sealing temperature and corresponding pressure profile during vacuum sealing process.

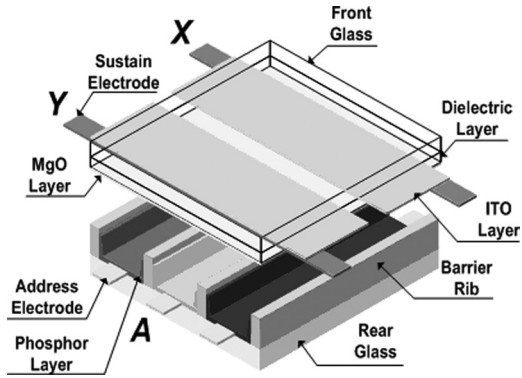

FIGURE 3 Schematic diagram of single pixel structure in 42-in. AC-PDP.

schematic diagram and the sealing process of the 42-in. AC-PDP panel fabricated by the vacuum sealing process. As shown in Figure 2(b), in the vacuum sealing method, the front and rear glasses were sealed under a high vacuum of about 10^{-5} Torr.

Figure 3 shows the single pixel structure of the 42-in. ac-PDP panel employed in this work. The detailed panel specifications are listed in Table 1.

3. EXPERIMENTAL OBSERVATION ON MgO CHARACTERISTICS OF VACUUM SEALING METHOD

3.1. Monitoring of Firing Voltages Measured for Discharge and Nondischarge Regions Using V_t Closed Curve Technique

Table 2 shows the variations in the firing voltages measured for the discharge and non-discharge regions under no initial wall charges

TABLE 1 Specifications of 42-in. AC-PDP Used in this Study

Front panel		Rear panel	
ITO width	225 μm	Barrier rib width	55 μm
ITO gap	85 μm	Barrier rib height	120 μm
Bus width	50 μm	Address width	95 μm
Pixel pitch		$912 \times 693\ \mu m^2$	
Gas chemistry		Ne-Xe (15%)-He (35%)	
Barrier rib type		Closed rib	

TABLE 2 Firing Voltages Measured for Discharge and Nondischarge Regions From Test Panels Fabricated by the Conventional and the Vacuum Sealing Methods

		Firing voltage			
		Conventional sealing method		Vacuum sealing method	
Region		Non-discharge region	Discharge region	Non-discharge region	Discharge region
MgO Cathode	I	272 V	242 V	246 V	256 V
	II	182 V	178 V	168 V	170 V
	III	206 V	208 V	196 V	192 V
	IV	306 V	318 V	294 V	290 V
Phosphor Cathode	V	344 V	290 V	332 V	228 V
	VI	340 V	280 V	328 V	216 V

where I : V_{tXY} (Discharge start threshold cell voltage between the X-Y electrodes), II: V_{tAY} (Discharge start threshold cell voltage between the A-Yelectrodes), III: V_{tAX} (Discharge start threshold cell voltage between the A-X electrodes), IV: V_{tYX} (Discharge start threshold cell voltage between the Y-X electrodes), V: V_{tYA} (Discharge start threshold cell voltage between the Y-A electrodes), and VI: V_{tXA} (Discharge start threshold cell voltage between the X-A) in the 42-in. panels fabricated by two different sealing methods such as the conventional and vacuum sealing methods. The discharge region is meant by displaying a square-type image (197×72 pixels) at half of peak luminance (about $500\,cd/m^2$) for about 1000 hours. Using the automatic power control (APC) system of the PDP, 760 sustain pulses were alternately applied to the X and Y electrodes during 1 TV field (16.67 ms) to display a square type test image with a 1% display region within the entire region of the 42-in. panel. The nondischarge region means that no discharge is produced. As shown in Table 2 and Figure 4(a) for the discharge region in the conventional sealing method, the firing voltages for side V (plate-gap discharge between the Y-A electrodes under the phosphor cathode condition) and VI (plate-gap discharge between the X-A electrodes under the phosphor cathode condition) were decreased by about 54–60 V than those of the nondischarge region. As shown in Table 2 and Figure 4(b) for the discharge region in the vacuum sealing method, the firing voltages for sides V and VI were remarkably decreased by about 104–112 V than those of the nondischarge region. The reduction in the firing voltage for the

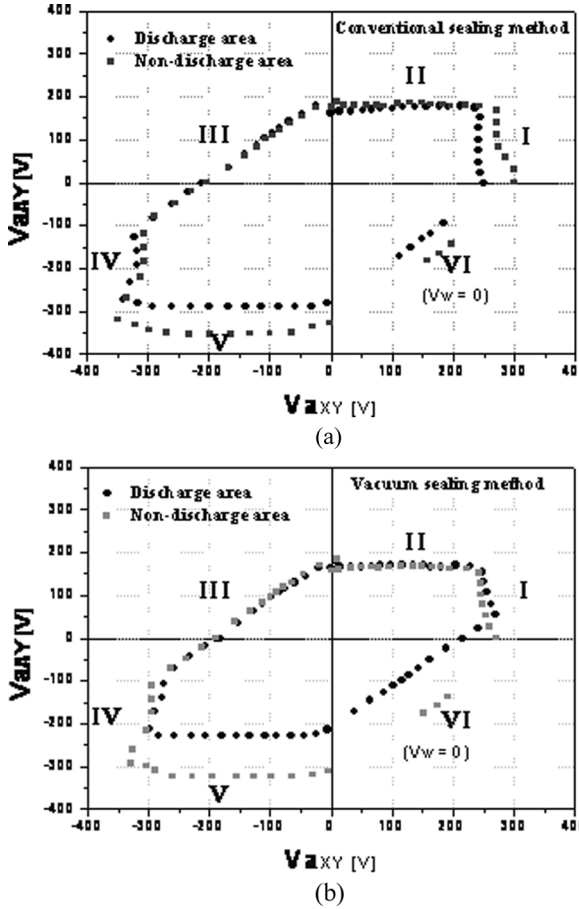

FIGURE 4 Comparison of V_t closed curves measured from discharge and non-discharge regions in (a) conventional and (b) vacuum sealing methods.

plate-gap discharge under the phosphor cathode conditions was mainly due to the deposition of Mg species onto the phosphor layer, caused by the sputtering of MgO induced by iterant strong sustain discharge [7]. As shown in Table 2 and Figure 4, the firing voltages of the phosphor cathode conditions (sides V and VI) in the discharge region for the vacuum sealing method were more decreased than those of the conventional sealing method. This result means that the redeposition of Mg species onto the phosphor layer for the vacuum sealing method was more increased than that of the conventional sealing method.

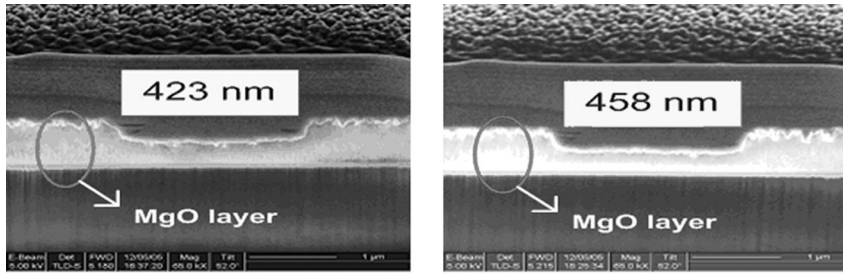

(a) (b)

FIGURE 5 Comparison of MgO sputtering rates in 42-in. panels (Xe: 15%) fabricated by both (a) conventional and (b) vacuum sealing methods using FIB.

3.2. Monitoring of Sputtering Rate and Hardness of MgO Layer

To identify why the Mg species are more deposited on the phosphor layer for the vacuum sealing method, both the focused ion beam (FIB) and nanoindentor were used to inspect the MgO sputtering rate and the MgO hardness, respectively.

Figure 5 shows the comparison of the SEM cross sectional morphologies of the sputtered MgO layer for the conventional and vacuum

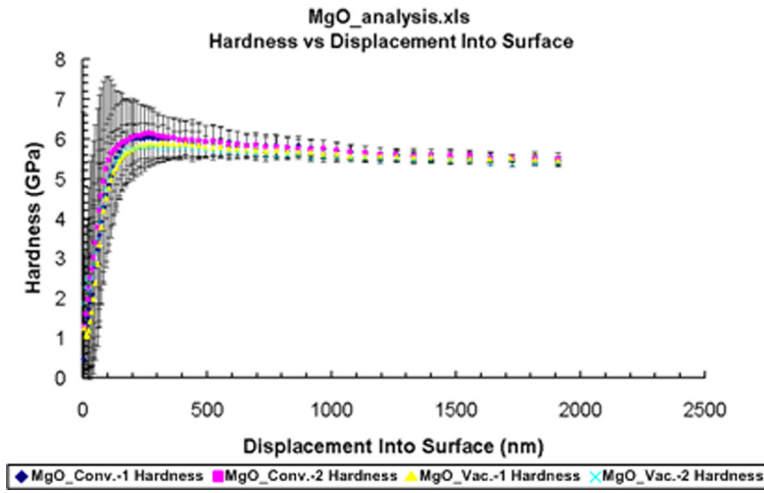

FIGURE 6 Comparison of MgO hardness in 42-in. panels (Xe: 15%) fabricated by both conventional and vacuum sealing methods using nano-indentor.

sealing methods respectively using the focused ion beam (FIB). The FIB meant the rate of the MgO sputtered from the MgO layer when Ga ions (30 keV) struck the surface of the MgO layer for 105 sec. The sputtering rate of the MgO layer for the vacuum sealing method was increased than the conventional sealing method.

Figure 6 shows the comparison of the hardness of the MgO layer for the conventional and the vacuum sealing methods using nanoindentor. In Figure 6, the nanoindentor means the digged depth and area of the MgO layer when the Berkovich indentation particle of nanosize pressed the surface of the MgO layer. The hardness of the MgO layer for the vacuum sealing method was more decreased than that of the conventional sealing method.

4. ANALYSIS ON MgO SURFACE CHANGE AND RELATED PHOTOLUMINESCENCE CHARACTERISTIC CHANGE CAUSED BY VACUUM SEALING METHOD

As shown in Table 3, in conventional sealing method, when the front and rear glasses are sealed under the high temperature and the atmospheric pressure (about 760 Torr), lots of oxygen may be included. However, in vacuum sealing method, when the front and rear glasses are sealed under the high temperature and the high vacuum (about 10^{-5} Torr), few oxygen may be included because of the high vacuum level. Consequently, the oxygen vacancy of the MgO layer for vacuum sealing method was increased than the conventional sealing method [8]. The 42-in. panel fabricated by the vacuum sealing method shows the changes in the MgO characteristics, such as firing voltage, MgO sputtering rate, and MgO hardness, which are caused by an increase in the oxygen vacancy of the MgO layer.

Figure 7 shows the comparison of photo intensity of the phosphor layers measured for the nondischarge and the discharge regions in the conventional and the vacuum sealing methods by photoluminescence (PL). The PL meant the photo intensity (visible rays, $300 \sim 780$ nm) emitted from the phosphor layers when the vacuum ultra

TABLE 3 Sealing Temperature and Pressure Between 42-inch Panels Fabricated by the Conventional and the Vacuum Sealing Methods

	Conventional sealing method	Vacuum sealing method
Sealing temperature	460°C	460°C
Sealing pressure	760 Torr	10^{-5} Torr

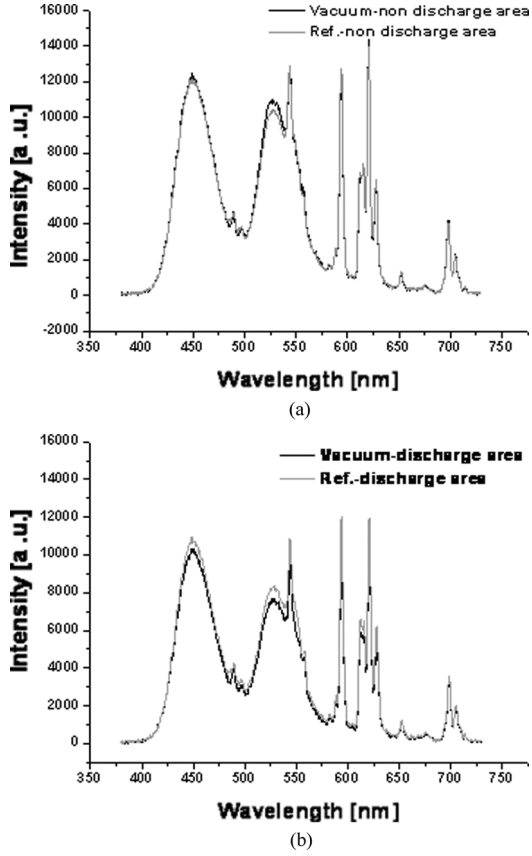

FIGURE 7 Comparison of photo-intensity of the phosphor layers measured for (a) non-discharge region and (b) discharge region from 42-inch panels fabricated by the conventional and the vacuum sealing methods using PL.

violet (VUV, 173 nm using the Kr ramp) irradiated the surface of the phosphor layers. The photo intensity of the phosphor layers measured for the nondischarge region in the conventional and the vacuum sealing methods are almost the same. However, the photo intensity of the phosphor layers measured for the discharge region in the vacuum sealing method was more deteriorated than the conventional sealing method. This indicates that the re-deposition of Mg spices onto the phosphor layer for the vacuum sealing method is increased than that of the conventional sealing method. The life-time of the MgO layer for vacuum sealing method was decreased than the conventional sealing method.

CONCLUSION

In this paper, the vacuum sealing method to enhance a base vacuum level is adopted, and the resultant changes (increase in the oxygen vacancy of the MgO layer) in the MgO characteristics, such as firing voltage, MgO sputtering rate, MgO hardness, and photoluminescence, were examined in comparison with the conventional sealing method in the 42-in. AC-PDP with a high Xe (15%) content. The life time of the MgO layer for the vacuum sealing method was more decreased than the conventional sealing method.

REFERENCES

[1] Kwon, S. J. & Jang, C.-K. (2004). *J. Information Display*, *5*(4), 7–11.
[2] Lee, D.-J., Moon, S.-I., Lee, Y.-H., & Ju, B.-K. (2001). *IMID'01, 1, 495–498.*
[3] Lee, D.-J., Moon, G.-J., Kim, J.-D., Song, C.-H., Jang, J., Oh, M.-H., & Ju, B.-K. (2002). *IDW'02, 9, 849–852.*
[4] Uchida, K., Uchida, G., Kurauchi, T., Terasawa, T., Kajiyama, H., & Shinoda, T. (2006). *IDW'06 Digest, 13, 347–350.*
[5] Park, C.-S., Tae, H.-S., Kwon, Y.-K., Seo, S. B., Heo, E. G., & Lee, B.-H. (2007). *SID'07, 38, 1434–1437.*
[6] Park, C.-S., Tae, H.-S., Kwon, Y.-K., Heo, E. G., & Lee, B.-H. (2007). *IMID'07, 1, 320–323.*
[7] Park, C.-S., Tae, H.-S., Kwon, Y.-K., & Heo, E. G. (2007). *IEEE Trans. Electron Devices*, *54*(6), 1315–1320.
[8] Kupfer, H., Kleinhempel, R., Richter, F., Peters, C., Krause, U., Kopte, T., & Cheng, T. (2006). *J. Vac. Sci. Technol. A*, *24*(1), 106–113.